

S.K. Ellika
R. Jain
S.C. Patel
L. Scarpace
L.R. Schultz
J.P. Rock
T. Mikkelsen

Role of Perfusion CT in Glioma Grading and Comparison with Conventional MR Imaging Features

BACKGROUND AND PURPOSE: Perfusion imaging using CT can provide additional information about tumor vascularity and angiogenesis for characterizing gliomas. The purpose of our study was to demonstrate the usefulness of various perfusion CT (PCT) parameters in assessing the grade of treatment-naïve gliomas and also to compare it with conventional MR imaging features.

MATERIALS AND METHODS: PCT was performed in 19 patients with glioma (14 high-grade gliomas and 5 low-grade gliomas). Normalized ratios of the PCT parameters (normalized cerebral blood volume [nCBV], normalized cerebral blood flow [nCBF], normalized mean transit time [nMTT]) were used for final analysis. Conventional MR imaging features of these tumors were assessed separately and compared with PCT parameters. Low- and high-grade gliomas were compared by using the nonparametric Wilcoxon 2-sample tests.

RESULTS: Mean nCBV in the high- and low-grade gliomas was 3.06 ± 1.35 and 1.44 ± 0.42 , respectively, with a statistically significant difference between the 2 groups ($P = .005$). Mean nCBF for the high- and low-grade gliomas was 3.03 ± 2.16 and 1.16 ± 0.36 , respectively, with a statistically significant difference between the 2 groups ($P = .045$). Cut points of >1.92 for nCBV (85.7% sensitivity and 100% specificity), >1.48 for nCBF (71.4% sensitivity and 100% specificity), and <1.94 for nMTT (92.9% sensitivity and 40% specificity) were found to identify the high-grade gliomas. nCBV was the single best parameter; however, using either nCBV of >1.92 or nCBF of >1.48 improved the sensitivity and specificity to 92.9% and 100%, respectively. The sensitivity and specificity for diagnosing a high-grade glioma with conventional MR imaging were 85.7% and 60%, respectively.

CONCLUSIONS: PCT can be used for preoperative grading of gliomas and can provide valuable complementary information about tumor hemodynamics, not available with conventional imaging techniques. nCBV was the single best parameter correlating with glioma grades, though using nCBF when nCBV was <1.92 improved the sensitivity. An nCBV threshold of >1.92 was found to identify the high-grade gliomas.

Gliomas, the most common primary brain neoplasms in adults, are very heterogeneous tumors. High-grade gliomas can be highly invasive and extremely vascular tumors.

Glioma grading is currently based on the histopathologic assessment of the tumor, which is achieved by stereotactic brain biopsy or cytoreductive surgery; and there are inherent limitations with these techniques and their interpretation.¹ Therapeutic approaches, response to therapy, and prognosis depend on accurate grading, and thus finding the part of the tumor with the highest grade to be biopsied is critical.

Conventional MR imaging has a limited role in differentiating gliomas because contrast-enhanced images reveal disrupted or absent blood-brain barrier and not necessarily microvasculature or neovascularity of the tumoral lesion.^{2,3} The 2 most important factors in determining the malignancy of gliomas is their ability to infiltrate the brain parenchyma and to recruit or synthesize vascular networks for further growth.⁴

Malignant brain tumors are characterized by neovascularity and increased angiogenic activity, with a higher proportion of immature and hyperpermeable vessels.^{5,6} Because vascular

proliferation is an important characteristic in the grading of astrocytomas,⁷ imaging techniques that provide hemodynamic information about the tumor may help in characterizing glioma malignancy, which may overcome some of the limitations of histopathologic sampling error and conventional MR imaging. Perfusion imaging has been useful in grading cerebral neoplasms⁸⁻¹⁴ and may provide reliable information on tumor physiology such as microvasculature, angiogenesis, micronecrosis, and cellularity.

Perfusion imaging of brain tumors has shown that certain cerebral perfusion parameters such as regional blood volume and blood flow correlate well with tumor grade, and it has also been helpful in distinguishing recurrent tumor from radiation necrosis.^{3,15}

Most of the prior perfusion studies comparing histologic features with perfusion parameters have used various MR perfusion techniques.^{3,15} However, recently perfusion CT (PCT) has been used as an alternative method in assessing cerebral hemodynamics for stroke and brain tumors.¹⁶ PCT allows measurement of tumor vascular physiology, and maps of tumor blood flow, blood volume, mean transit time (MTT), and permeability–surface area product can be generated. In view of the wider availability, faster scanning times, and low cost combined with its ease of quantification of various perfusion parameters as compared with MR perfusion, PCT is potentially well suited to studying brain tumors and monitoring tumor response to antiangiogenic agents.¹⁶

The purpose of our study was to demonstrate the useful-

Received October 20, 2006; accepted after revision April 23, 2007.

From the Division of Neuroradiology, Department of Radiology (S.K.E., R.J., S.C.P.), Departments of Neurology and Neurosurgery (L.S., J.P.R., T.M.), and Biostatistics and Research Epidemiology (L.R.S.), Henry Ford Health System, Detroit, Mich.

Please address correspondence to: Rajan Jain, MD, Division of Neuroradiology, Department of Radiology, Henry Ford Health System, 2799 West Grand Blvd, Detroit MI 48202; e-mail rajanj@rad.hfh.edu

DOI 10.3174/ajnr.A0688

Table 1: Patient demographics with MR imaging features and PCT measurements

No.	Age/ Sex	Contrast					Signal Heterogeneity	Involvement					nCBV	nCBF	nMTT
		Enhance- ment	Hemorr- hage	Necro- sis	Vasogenic Edema	Mass Effect		of Corpus Callosum	Crossing Midline	MR Grade of Tumor	WHO Grade of Tumor				
1	20/M	HE	-	-	+	+	HT	+	+	HG	I	1.92	0.58	3.55	
2	27/F	NCE	-	-	+	+	HO	-	-	LG	II	1.07	1.48	0.83	
3	34/M	NCE	-	CD	+	++	HT	+	+	LG	II	0.94	1.26	1.07	
4	56/F	HE	-	+	++	++	HT	-	-	HG	II	1.56	1.07	1.94	
5	34/F	NCE	-	-	-	+	HO	-	-	LG	II	1.72	1.43	1.08	
6	18/F	HE	-	+	-	+	HT	-	-	HG	III	2.26	1.53	1.41	
7	39/M	HE	-	+	+	+	HT	-	-	HG	III	2.21	1.23	1.71	
8	57/M	HE	+	+	+	+++	HT	-	-	HG	III	5.39	6.84	2.63	
9	68/M	NCE	-	+	+	+	HT	-	-	LG	III	3.7	3.75	0.92	
10	39/F	HE	+	+	++	+++	HT	+	+	HG	III	2.61	1.65	1.68	
11	34/M	NCE	-	CD	-	++	HT	+	+	LG	III	1.5	0.78	1.32	
12	64/M	PNE	+	+	++	+++	HT	+	+	HG	IV	1.96	1.19	1.78	
13	39/F	PNE	-	+	++	+++	HT	+	-	HG	IV	2.05	1.07	1.51	
14	55/F	PNE	-	+	++	+++	HT	+	+	HG	IV	3.95	2.87	1.11	
15	60/M	PNE	+	+	+++	+++	HT	+	-	HG	IV	2.86	2.49	0.74	
16	69/M	PNE	-	+	+	++	HT	-	-	HG	IV	1.12	1.69	1.04	
17	66/F	HE	-	+	+	+	HT	+	-	HG	IV	5.3	6.16	0.77	
18	46/M	HE	+	+	++	++	HT	+	+	HG	IV	4.3	6.27	0.63	
19	57/M	PNE	-	+	+++	+++	HT	-	-	HG	IV	3.61	4.91	0.83	

Note:—HE indicates heterogeneous enhancement; NCE, no contrast enhancement; PNE, peripheral nodular enhancement; CD, cystic degeneration; HT, heterogenous; HO, homogeneous; HG, high grade; LG, low grade; +, present; -, absent.

ness of various PCT parameters such as cerebral blood volume (CBV), cerebral blood flow (CBF), and MTT in assessing the grade of treatment-naïve gliomas and also to compare them with conventional MR features.

Materials and Methods

The Study Group

Our institutional review board approved this prospective study, and an informed consent was obtained from each participant before the study. The study group consisted of 19 patients, 11 men and 8 women, ranging in age from 18–69 years (mean age, 46.4 years) with treatment-naïve brain tumors, of which 5 were biopsy-proved low-grade gliomas (World Health Organization [WHO] grade I, $n = 1$ and grade II, $n = 4$), and 14 had high-grade gliomas (WHO grade III, $n = 6$ and grade IV, $n = 8$). We did not have any pilocytic astrocytomas in the low-grade group. Histopathologic evaluation was based on the WHO system; grade I and II, low-grade glioma; grade III, anaplastic glioma; and grade IV, glioblastoma multiforme (GBM). All patients underwent PCT before any treatment. Cytoreductive surgery (subtotal resection in 16 patients and gross total resection in 1 patient) was performed in 17 patients, and histopathologic diagnosis in this subset of patients was obtained from surgical specimens. Two patients underwent stereotactic biopsy without surgical resection of the tumor. The tumor area ranged from 2.06 to 61.08 cm² (mean, 21.95 cm²) measured on postcontrast T1-weighted MR images. The tumor area for the nonenhancing tumors was measured by using the area of T1 hypointensity on the postcontrast scans.

Conventional MR Imaging

Imaging was performed with a 3T unit (Signa Excite HD; GE Healthcare, Milwaukee, Wis). A localizing sagittal T1-weighted image (3196/6 [TR/TE]) was obtained, followed by nonenhanced axial T1-weighted (3000/6 [TR/TE]), axial fluid-attenuated inversion recovery (10 002/120/2550 [TR/TE/TI]), and T2-weighted (3000/103[TR/TE]) images. Contrast-enhanced axial T1-weighted imaging was also performed (3000/6 [TR/TE]).

One experienced neuroradiologist (S.C.P), blinded to the PCT results, reviewed the conventional MR images and graded each tumor according to the 2-tier imaging grading system: low- versus high-grade gliomas. Grading of tumors on conventional MR imaging was based on 8 criteria: contrast material enhancement, mass effect, signal-intensity heterogeneity, hemorrhage, necrosis, degree of edema, involvement of the corpus callosum, and crossing of the midline.^{17,18} The degree of vasogenic edema was further subclassified as 1+ (mild edema), 2+ (moderate edema), and 3+ (severe edema). Patient demographics and conventional MR imaging findings are included in Table 1.

PCT Technique

Perfusion studies were performed with a 16-section multidetector row CT scanner (LightSpeed; GE Healthcare). The most recent MR imaging studies of the patient were reviewed before the perfusion study. A noncontrast CT head scan was obtained to localize the region of interest before obtaining a perfusion scan. For the perfusion scan, 50 mL of nonionic contrast (300 mg I/mL) was injected at a rate of 4 mL/s through a 20-gauge intravenous line. At 5 seconds into the injection, a cine (continuous) scan was initiated with the following technique: 80 kVp, 190–200 mA, 4 × 5 mm sections, and 1 second per rotation for a duration of 50 seconds. The 1-second images were reformatted at 0.5-second intervals, and the 5-mm sections were reformatted into two 10-mm-thick sections. Perfusion maps of CBV, CBF, and MTT were generated at an Advantage Windows workstation by using the PCT 3.0 software (GE Healthcare) in all patients. We used the superior sagittal sinus as the venous output function in all patients and the artery with the greatest peak and slope on time-attenuation curves as the arterial input function.

The contralateral anterior cerebral artery as the arterial input function was used in 17 patients, and the contralateral middle cerebral artery was used in 1 patient for generation of the perfusion maps. All patients tolerated PCT without any adverse reactions to the rapid-bolus injection of contrast.

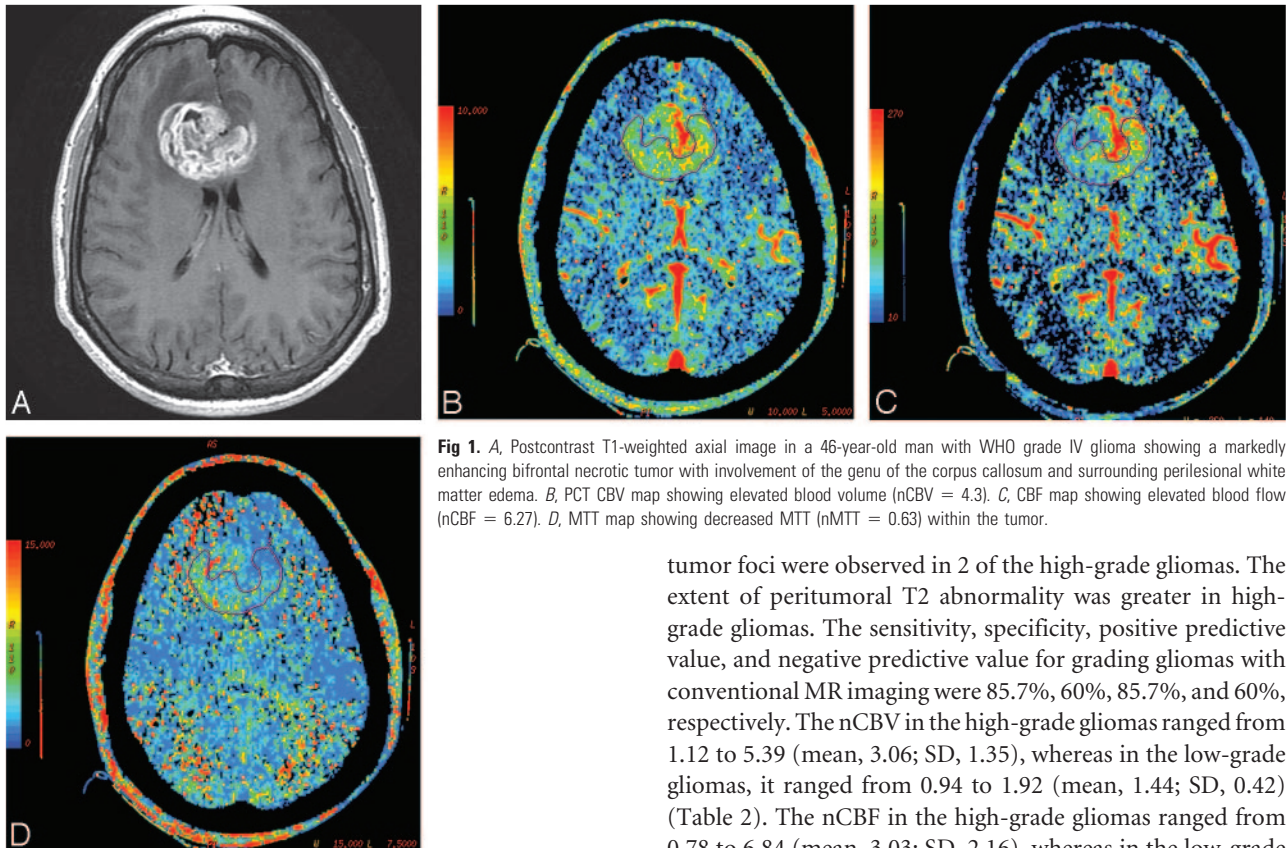


Fig 1. A, Postcontrast T1-weighted axial image in a 46-year-old man with WHO grade IV glioma showing a markedly enhancing bifrontal necrotic tumor with involvement of the genu of the corpus callosum and surrounding perilesional white matter edema. B, PCT CBV map showing elevated blood volume (nCBV = 4.3). C, CBF map showing elevated blood flow (nCBF = 6.27). D, MTT map showing decreased MTT (nMTT = 0.63) within the tumor.

Perfusion Data Processing

In the quantitative assessment, manually drawn regions of interest were placed in the tumor, and the absolute perfusion parameter values were recorded. CBV, CBF, and MTT were normalized (nCBV, nCBF, nMTT) by dividing tumor absolute perfusion parameter values by values obtained from the normal-appearing white matter of the contralateral cerebral hemisphere as far away from the primary neoplasm as possible. We placed the regions of interest in the solid portion of the tumor, taking care to avoid necrosis or areas of cystic degeneration (Figs 1–3).

Statistical Analysis

Low- and high-grade tumors were compared by using the nonparametric Wilcoxon 2-sample test. This test is similar to the Student 2-sample *t* test but does not require the assumption of equal variability between the 2 groups. Receiver operating characteristic analysis curves for each perfusion parameter were computed to identify the cut points that maximized the sum of sensitivity and specificity. In this analysis, “sensitivity” was defined as the proportion of correctly identified high-grade tumors, and “specificity” was defined as the proportion of correctly identified low-grade tumors.

Results

Fourteen of the 19 patients had high-grade gliomas, and 5 had low-grade gliomas. Table 1 summarizes the findings of the morphologic MR imaging features in all the 19 patients.

All except 2 of the high-grade gliomas and 3 of the low-grade gliomas showed contrast enhancement. All GBMs in the high-grade group showed necrosis. Of the high-grade gliomas, 5 had hemorrhage, and none of the low-grade gliomas showed foci of hemorrhage. Multifocal tumors with distant areas of

tumor foci were observed in 2 of the high-grade gliomas. The extent of peritumoral T2 abnormality was greater in high-grade gliomas. The sensitivity, specificity, positive predictive value, and negative predictive value for grading gliomas with conventional MR imaging were 85.7%, 60%, 85.7%, and 60%, respectively. The nCBV in the high-grade gliomas ranged from 1.12 to 5.39 (mean, 3.06; SD, 1.35), whereas in the low-grade gliomas, it ranged from 0.94 to 1.92 (mean, 1.44; SD, 0.42) (Table 2). The nCBF in the high-grade gliomas ranged from 0.78 to 6.84 (mean, 3.03; SD, 2.16), whereas in the low-grade gliomas, it ranged from 0.58 to 1.48 (mean, 1.16; SD, 0.36). The nMTT in the high-grade gliomas ranged from 0.63 to 2.63 (mean, 1.29; SD, 0.55), whereas in the low-grade gliomas, it ranged from 0.83 to 3.55 (mean, 1.69; SD, 1.12). The difference in nCBV and nCBF between the 2 groups was statistically significant ($P = .005$ and $P = .045$, respectively), with patients with low-grade tumors having a lower mean nCBV and nCBF than patients with high-grade tumors. No statistically significant difference was observed between the 2 groups for nMTT ($P = .559$); however, the trend was for lower nMTT in high-grade gliomas.

For nCBV, the cut point of >1.92 was selected to identify high-grade tumors (85.7% sensitivity and 100% specificity) (Fig 4). For nCBF, the cut point of >1.48 was selected to identify high-grade tumors (71.4% sensitivity and 100% specificity) (Fig 5).

The cut point selected for nMTT was <1.94 for high-grade tumors (92.9% sensitivity and 40% specificity) (Fig 6). Table 3 shows the results of the sensitivity/specificity analyses. The high-grade gliomas were divided into 2 groups (grade III and grade IV), and pairwise comparisons were performed between the low-grade and high-grade tumors and also between the 2 subgroups of the high-grade gliomas for differences in nCBV, nCBF, and nMTT. The differences in nCBV between low-versus-grade III and low-versus-grade IV gliomas were statistically significant ($P = .03$ and $P = .01$, respectively); however, there was no statistically significant difference between grade III and grade IV ($P > .05$). In addition, the difference between low-grade and grade IV for nCBF was also significant ($P = .048$). No other differences between tumor groups for nCBF or nMTT were observed ($P > .05$) (Table 2).

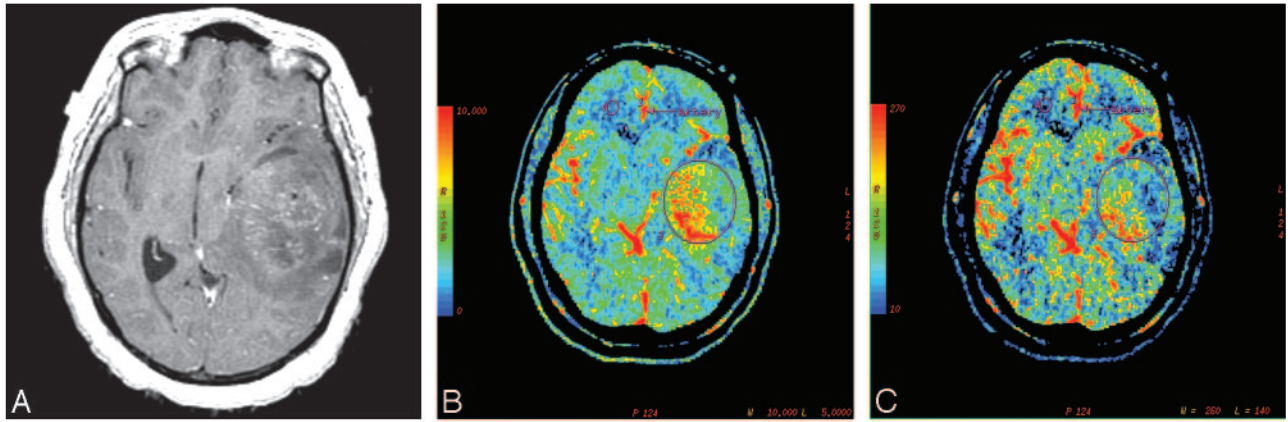


Fig 2. WHO grade III glioma in a 39-year-old woman. *A*, Postcontrast T1-weighted axial image showing a large heterogeneously enhancing left temporal mass lesion with significant mass effect. *B*, Corresponding CBV map showing elevated blood volume (nCBV = 2.61). *C*, CBF map showing increased blood flow (nCBF = 1.65). *D*, MTT map showing decreased MTT (nMTT = 1.68) within the tumor. Also note the mismatch between areas of increased blood volume/blood flow on the CBV/CBF maps and the areas of gadolinium enhancement.

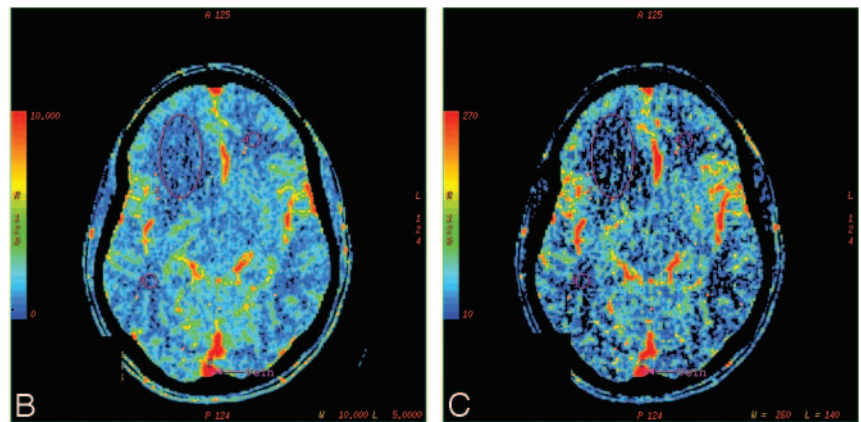
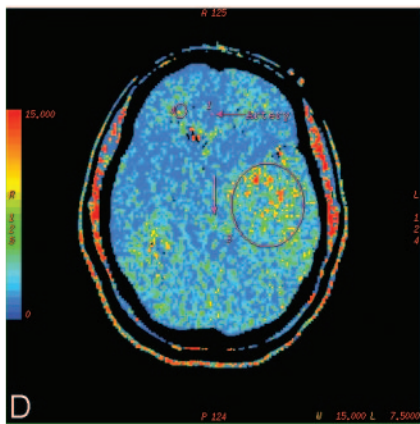


Fig 3. A 34-year-old man with WHO grade II glioma. *A*, Postcontrast T1-weighted axial image showing a nonenhancing mass in the right frontal lobe. *B*, CBV map showing low blood volume (nCBV = 0.94). *C*, CBF map showing decreased blood flow (nCBF = 1.26). *D*, MTT map showing increased transit time (nMTT = 1.07) within the tumor.

Discussion

Gliomas are histologically very heterogeneous, with varying degrees of cellular and nuclear pleomorphism, mitotic activity, vascular proliferation, and necrosis.¹⁹⁻²¹

There are significant limitations associated with histopathologic grading, which include sampling errors,²² wide range of classification and grading systems used for brain tumors, inter- and intrapathologist variability, and the changing nature of central nervous system tumors.^{23,24} The degree of vascular proliferation is one of the most critical elements in the determination of tumor grade and prognosis, thus preoperative noninvasive assessment of glioma vascularity can be helpful in determining the malignant potential of the tumor, in selection of an appropriate biopsy site, in predicting transition

Table 2: PCT parameters and P values for the various subgroups

Group (No. of Patients)	nCBV	nCBF	nMTT
	Mean (SD)	Mean (SD)	Mean (SD)
Low Grade (5)	1.44 (0.42)	1.16 (0.36)	1.69 (1.12)
High Grade (III and IV) (14)	3.06 (1.35)	3.03 (2.16)	1.29 (0.55)
P value	0.005	0.045	0.559
Grade III (6)	2.95 (1.39)	2.63 (2.30)	1.61 (0.58)
Grade IV (8)	3.14 (1.40)	3.33 (2.15)	1.05 (0.40)
P value for Low vs III	0.03	0.177	0.792
P value for Low vs IV	0.01	0.048	0.222
P value for III vs IV	0.949	0.572	0.081

Normalized CBV values

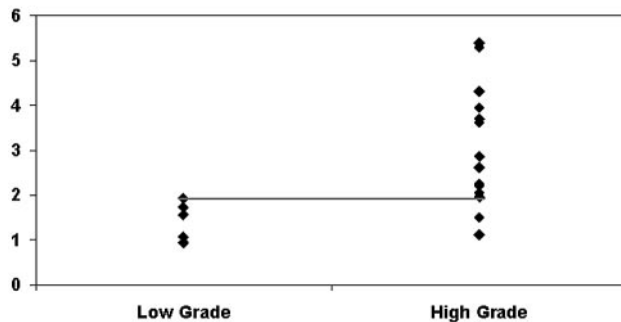


Fig 4. Scatter plot for nCBV versus grade of tumor showing the threshold to differentiate low- from high-grade tumors.

Normalized CBF values

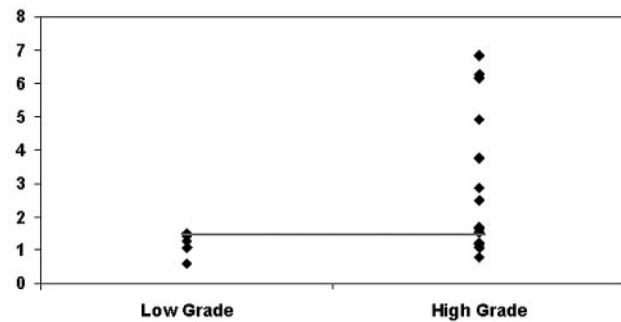


Fig 5. Scatter plot for nCBF versus grade of tumor showing the threshold to differentiate low- from high-grade tumors.

from low-grade to a high-grade glioma, and also in monitoring response to various treatment modalities.²⁵⁻²⁷

Conventional MR imaging provides important anatomic information; however, it is insufficient in determining the grade of the tumors preoperatively.¹⁷ Contrast enhancement on MR imaging depicts areas of breakdown of blood-brain barrier,²⁸ which is often associated with higher tumor grade; however, contrast enhancement is not always accurate in predicting the tumor grade.^{8,29-32} Even in the high-grade gliomas with pathologic contrast enhancement, the enhancement may not reflect the areas of neovascularity and angiogenesis.^{33,34} Thus radiologic grading of tumors with conventional MR imaging is not always accurate, with sensitivity in identifying

Normalized MTT values

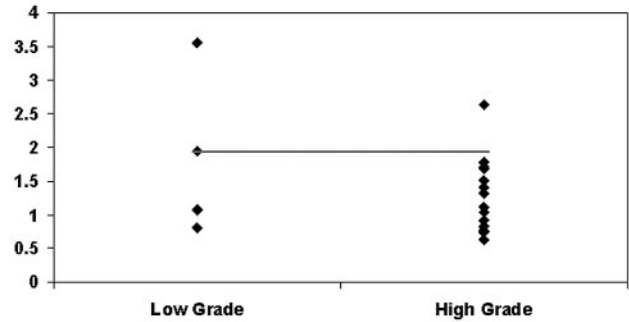


Fig 6. Scatter plot for nMTT versus grade of tumor showing the threshold to differentiate low- from high-grade tumors.

high-grade gliomas ranging from 55.1% to 83.3% in various studies^{8,14,17,18,31} and 85.7% in our study. Finally, conventional MR imaging does not provide information on tumor physiology, which is also an important factor in determining the tumor grade.

Vast arrays of noninvasive imaging techniques have been used to detect and grade malignancy, which include positron-emission tomography, MR spectroscopy, MR diffusion and perfusion imaging, as well as various image-processing methods; however, no single method alone has been shown to be reliable in grading brain tumors.^{2,35-38}

Because angiogenesis is an important feature in malignant gliomas, perfusion imaging may provide additional important information. An overall principle of perfusion oncologic imaging is that with tumor growth, its metabolic demands increase due to rapid cell growth and cell turnover. Cellular hypoglycemia and hypoxia lead to the production of angiogenic cytokines, which leads to neoangiogenesis, which in turn increases the capillary attenuation within the tumor.³⁹ Increased capillary attenuation leads to higher blood volume and blood flow in the tumor bed.^{39,40}

Perfusion studies, especially by using MR imaging techniques, have been used to noninvasively estimate tumor grade preoperatively.^{11,39,40} PCT has been used extensively in evaluation of stroke and can serve as an alternative method for assessing tumor hemodynamics. This method has been validated in animal and human studies.⁴¹⁻⁴⁴

The increasing number of publications reporting a correlation between hemodynamic parameters and histologic measurements of angiogenesis, such as microvessel density, validate the use of PCT as a marker of angiogenesis.⁴¹⁻⁴⁵

Perfusion imaging of brain tumors, which has mostly used various MR perfusion techniques, can also be used for stereotactic biopsy guidance,¹¹ better delineation of tumor margins,^{9,38} and also for assessing treatment response.^{15,46} PCT shares the advantages of MR perfusion and potentially has advantages over MR perfusion because of easy accessibility, measurement of absolute perfusion values, and relatively easy postprocessing. In addition, there are some important limitations associated with MR perfusion: 1) The technique is susceptibility-weighted. It is extremely sensitive to magnetic field inhomogeneity, and thus hemorrhagic products can complicate the analysis. 2) The cost of imaging hardware can

Table 3: Sensitivity and specificity analyses using perfusion parameter thresholds

Criteria	High Grade		Low Grade	
	Sensitivity	95% CI	Specificity	95% CI
nCBV >1.92	85.7% (12/14)	(57.2%–98.2%)	100% (5/5)	(47.8%–100%)
nCBF >1.48	71.4% (10/14)	(41.9%–91.6%)	100% (5/5)	(47.8%–100%)
nMTT <1.94	92.9% (13/14)	(66.1%–99.8%)	40% (2/5)	(5.3%–85.3%)
nCBV >1.92 or nCBF >1.48	92.9% (13/14)	(66.1%–99.8%)	100% (5/5)	(47.8%–100%)

Note:—CI indicates confidence interval.

be high because perfusion MR imaging requires high-performance gradients and very fast echo-planar imaging sequences. 3) Calculation of rCBV can be inaccurate in lesions such as GBM or meningioma, where there is a severe breakdown or absence of the blood-brain barrier.⁴⁷ 4) Perfusion measurements are relative rather than absolute values. However, limitations of PCT include the radiation dose involved with the procedure and the limited coverage area compared with MR perfusion.

The correlation between the histopathologic grade of cerebral gliomas and rCBV has been evaluated several times with perfusion MR imaging studies, which have shown mean rCBV ratios of high-grade gliomas to range between 3.64 and 7.32, which are significantly different from those of low-grade gliomas, which range between 1.11 and 2.14.^{3,8,12,14,15,48} In our study, mean nCBV of the high- and low-grade gliomas was 3.06 and 1.44, respectively ($P = .005$). The values for the low-grade gliomas in our study are in concordance with other perfusion studies; however, the values for the high-grade tumors are less than the values observed with MR perfusion in the literature. Similar lesser CBV and CBF values were described with PCT by Eastwood and Provenzale⁴⁹ and were hypothesized to be due to differences in microvasculature of the tumors, scaling factor differences, and better correction for the effects of contrast leakage with PCT⁴³ and probably erroneous overestimation of the CBF and CBV with MR perfusion. The same factors could be at play in our study, giving us lower nCBV compared with previous MR perfusion studies. We also analyzed grade III and grade IV tumors separately and found no statistical difference between these 2 grades, and our findings are in concordance with other imaging studies that failed to differentiate between these 2 subgroups.^{12,14}

Previous studies using MR perfusion have described various rCBV threshold values. Lev and Rosen¹¹ described a threshold of 1.5 in discriminating between patients with low- and high-grade gliomas, with a sensitivity and specificity of 100% and 69%, respectively.

Law et al¹⁴ showed a sensitivity and specificity of 95.0% and 57.5%, respectively, by using 1.75 as the threshold value. Shin et al¹² used a threshold of 2.93, with a sensitivity of 90.9% and a specificity of 83.3%. Hakyemez et al⁴⁸ used a threshold of 2.00 to differentiate low- and high-grade gliomas, with 100% sensitivity and 90.9% specificity. Using an nCBV of >1.92 (sensitivity of 85.7% and specificity of 100%), we were able to identify all the low-grade tumors, but 2 of the high-grade tumors were misclassified (nCBV of 1.5 and 1.12). Using either an nCBV of >1.92 or an nCBF of >1.48, PCT misclassified only 1 case, which was misclassified on MR imaging too, thus slightly improving the sensitivity of PCT to 92.9%, and the specificity remained 100%. This sensitivity and specificity of PCT appear to be better than those defined by previous studies.

In this study, conventional MR imaging misclassified 4 cases (low-grade glioma, $n = 2$ and high-grade glioma, $n = 2$), of which both the low-grade gliomas and 1 high-grade glioma were correctly classified with PCT. One high-grade glioma, which was misclassified by both PCT and conventional MR imaging, was a diffuse tumor involving both the cerebral hemispheres, and the low nCBV values can be explained by intermingling of the tumor cells with the normal neurons and white matter tracts, leading to the lower observed values. Another interesting finding in our study was the mismatch between the areas of contrast enhancement and areas of high CBV on the perfusion maps in 4 patients. This is not surprising because areas of contrast enhancement are caused by alteration or break in the blood-brain barrier with or without vascular hyperplasia, whereas perfusion abnormality reflects the degree of tumor vascularity and tumor angiogenesis.

Limitations of our study include the following: 1) the small number of patients, especially those with the low-grade gliomas; 2) the questionable reproducibility of the absolute values and variation in the absolute values of the PCT parameters obtained by using a different arterial input and venous output function for which we tried to compensate by using normalized ratios, normalized to the normal white matter rather than by using the absolute values; 3) One-to-one correlation between histologic specimen and abnormality seen on perfusion images or conventional MR images was not done.

Conclusions

PCT can be used for preoperative grading of gliomas. Because there may be an error in classifying these tumors on the basis of morphologic MR imaging features alone, PCT can provide complementary information about tumor vascularity of gliomas, which can be useful in predicting prognosis and tumor response to various antiangiogenesis therapies. nCBV was the single best parameter correlating with glioma grades, though using nCBF when nCBV was <1.92 slightly improved the sensitivity in diagnosing high-grade gliomas.

PCT maps can also be very useful for surgical biopsy and/or radiosurgery guidance to target the areas of increased CBV, with a better histologic yield and better response to treatment. The sensitivity and specificity of PCT in tumor grading are not currently matched by any other imaging technique. These data may justify the more routine use of this technique in the assessment and follow-up of patients with gliomas.

References

1. Law M, Yang S, Babb JS, et al. Comparison of cerebral blood volume and vascular permeability from dynamic susceptibility contrast-enhanced perfusion MR imaging with glioma grade. *AJNR Am J Neuroradiol* 2004;25:746–55
2. Law M, Cha S, Knopp EA, et al. High-grade gliomas and solitary metastases: differentiation by using perfusion and proton spectroscopic MR imaging. *Radiology* 2002;222:715–21

3. Aronen HJ, Gazit IE, Louis DN, et al. **Cerebral blood volume maps of gliomas: comparison with tumour grade and histologic findings.** *Radiology* 1994;191:41–51
4. Folkman J. **The role of angiogenesis in tumor growth.** *Semin Cancer Biol* 1992;3:65–71
5. Nugent LJ, Jain RK. **Extravascular diffusion in normal and neoplastic tissues.** *Cancer Res* 1984;44:238–44
6. Jain RK, Gerlowski LE. **Extravascular transport in normal and tumor tissues.** *Crit Rev Oncol Hematol* 1986;5:115–70
7. Burger PC, Vogel FS. **The brain tumors.** In: Burger PC, Vogel FS, eds. *Surgical Pathology of the Central Nervous System and its Coverings.* New York: Wiley; 1982:223–66
8. Knopp EA, Cha S, Johnson G, et al. **Glial neoplasms: dynamic contrast-enhanced T2*-weighted MR imaging.** *Radiology* 1999;211:791–98
9. Wong JC, Provenzale JM, Petrella JR. **Perfusion MR imaging of brain neoplasms.** *AJR Am J Roentgenol* 2000;174:1147–57
10. Cha S, Knopp EA, Johnson G, et al. **Intracranial mass lesions: dynamic contrast-enhanced susceptibility-weighted echo-planar perfusion MR imaging.** *Radiology* 2002;223:11–29
11. Lev MH, Rosen BR. **Clinical applications of intracranial perfusion MR imaging.** *Neuroimaging Clin N Am* 1999;9:309–31
12. Shin JH, Lee HK, Kwun BD, et al. **Using relative cerebral blood flow and volume to evaluate the histopathologic grade of cerebral gliomas: preliminary results.** *AJR Am J Roentgenol* 2002;179:783–89
13. Petrella JR, Provenzale JM. **MR perfusion imaging of the brain: techniques and applications.** *AJR Am J Roentgenol* 2000;175:207–19
14. Law M, Yang S, Wang H, et al. **Glioma gradings: specificity and predictive values of perfusion MR imaging and proton MR spectroscopic imaging compared with conventional MR imaging.** *AJNR Am J Neuroradiol* 2003;24:1989–98
15. Sugahara T, Korogi Y, Tomiguchi S, et al. **Posttherapeutic intraaxial brain tumor: the value of perfusion-sensitive contrast-enhanced MR imaging for differentiating tumor recurrence from nonneoplastic contrast-enhancing tissue.** *AJNR Am J Neuroradiol* 2000;21:901–09
16. Miles KA, Charnsangavej C, Lee F, et al. **Application of CT in the investigation of angiogenesis in oncology.** *Acad Radiol* 2000;7:840–50
17. Dean BL, Drayer BP, Bird CR, et al. **Gliomas: classification with MR imaging.** *Radiology* 1990;174:411–15
18. Watanabe M, Tanaka R, Takeda N. **Magnetic resonance imaging and histopathology of cerebral gliomas.** *Neuroradiology* 1992;34:463–69
19. Burger PC, Vogel FS, Green SB, et al. **Glioblastoma multiforme and anaplastic astrocytoma: pathologic criteria and prognostic implications.** *Cancer* 1985;56:1106–11
20. Burger PC. **Malignant astrocytic neoplasms: classification, pathologic anatomy, and response to therapy.** *Semin Oncol* 1986;13:16–26
21. Burger PC, Scheithauer BW. *Tumors of the Central Nervous System.* Washington, DC: Armed Forces Institute of Pathology; 1994:452
22. Kelly PJ, Daumas-Duport C, Scheithauer BW, et al. **Stereotactic histologic correlations of computed tomography and magnetic resonance imaging-defined abnormalities in patients with glial neoplasms.** *Mayo Clin Proc* 1987;62:450–59
23. Jackson RJ, Fuller GN, Abi-Said D, et al. **Limitations of stereotactic biopsy in the initial management of gliomas.** *Neuro-oncol* 2001;3:193–200
24. Gilles FH, Brown WD, Leviton A, et al. **Limitations of the World Health Organization classification of childhood supratentorial astrocytic tumor: Children Brain Tumor Consortium.** *Cancer* 2000;88:1477–83
25. Wesseling P, Ruiters DJ, Burger PC. **Angiogenesis in brain tumors: pathobiological and clinical aspects.** *J Neurooncol* 1997;32:253–65
26. Johnson JP, Bruce JN. **Angiogenesis in human gliomas: prognostic and therapeutic implications.** In: Rosen EM, Goldberg D, eds. *Regulation of Angiogenesis.* Basel, Switzerland: Birkhauser; 1997:29–46
27. Lund EL, Spang-Thomsen M, Skovgaard-Poulsen H, et al. **Tumor angiogenesis: a new therapeutic target in gliomas.** *Acta Neurol Scand* 1998;97:52–62
28. Runge VM, Clanton JA, Price AC, et al. **The use of Gd DTPA as a perfusion agent and marker of blood-brain barrier disruption.** *Magn Reson Imaging* 1985;3:43–55
29. Ginsberg LE, Fuller GN, Hashmi M, et al. **The significance of lack of MR contrast enhancement of supratentorial brain tumors in adults: histopathological evaluation of a series.** *Surg Neurol* 1998;49:436–40
30. Perez-Cruet MJ, Adelman L, Anderson M, et al. **CT-guided stereotactic biopsy of nonenhancing brain lesions.** *Stereotact Funct Neurosurg* 1993;61:105–17
31. Kondziolka D, Lunsford LD, Martinez AJ. **Unreliability of contemporary neurodiagnostic imaging in evaluating suspected adult supratentorial (low-grade) astrocytoma.** *J Neurosurg* 1993;79:533–36
32. Mihara F, Numaguchi Y, Rothman M, et al. **Non-contrast-enhancing supratentorial malignant astrocytoma: MR features and possible mechanisms.** *Radiat Med* 1995;13:11–17
33. Bagley LJ, Grossman RI, Judy KD, et al. **Gliomas: correlation of magnetic susceptibility artifact with histologic grade.** *Radiology* 1997;202:511–16
34. Siegal T, Rubinstein R, Tzuk-Shina T, et al. **Utility of relative cerebral blood volume mapping derived from perfusion magnetic resonance imaging in the routine follow up of brain tumours.** *J Neurosurg* 1997;86:22–27
35. Shimizu H, Kumabe T, Tominaga T, et al. **Noninvasive evaluation of malignancy of brain tumors with proton MR spectroscopy.** *AJNR Am J Neuroradiol* 1996;17:737–47
36. Tamiya T, Kinoshita K, Ono Y, et al. **Proton magnetic resonance spectroscopy reflects cellular proliferative activity in astrocytomas.** *Neuroradiology* 2000;42:333–38
37. Yang D, Korogi Y, Sugahara T, et al. **Cerebral gliomas: prospective comparison of multivoxel 2D chemical-shift imaging proton MR spectroscopy, echoplanar perfusion and diffusion-weighted MRI.** *Neuroradiology* 2002;44:656–66
38. Henry RG, Vigneron DB, Fischbein NJ, et al. **Comparison of relative cerebral blood volume and proton spectroscopy in patients with treated gliomas.** *AJNR Am J Neuroradiol* 2000;21:357–66
39. Jackson A, Kassner A, Annesley-Williams D, et al. **Abnormalities in the recirculation phase of contrast agent bolus passage in cerebral gliomas: comparison with relative blood volume and tumor grade.** *AJNR Am J Neuroradiol* 2002;23:7–14
40. Covarrubias DJ, Rosen BR, Lev MH. **Dynamic magnetic resonance perfusion imaging of brain tumors.** *Oncologist* 2004;9:528–37
41. Cenic A, Nabavi DG, Craen RA, et al. **Dynamic CT measurement of cerebral blood flow: a validation study.** *AJNR Am J Neuroradiol* 1999;20:63–73
42. Cenic A, Nabavi DG, Craen RA, et al. **A CT method to measure hemodynamics in brain tumors: validation and application of cerebral blood flow maps.** *AJNR Am J Neuroradiol* 2000;21:462–70
43. Nabavi DG, Cenic A, Craen RA, et al. **CT assessment of cerebral perfusion: experimental validation and initial clinical experience.** *Radiology* 1999;213:141–49
44. Wintermark M, Thiran JP, Maeder P, et al. **Simultaneous measurement of regional cerebral blood flow by perfusion CT and stable xenon CT: a validation study.** *AJNR Am J Neuroradiol* 2001;22:905–14
45. Ding B, Ling HW, Chen KM, et al. **Comparison of cerebral blood volume and permeability in preoperative grading of intracranial glioma using CT perfusion imaging.** *Neuroradiology* 2006;48:773–81
46. Hazle JD, Jackson EF, Schomer DF, et al. **Dynamic imaging of intracranial lesions using fast spin-echo imaging: differentiation of brain tumors and treatment effects.** *J Magn Reson Imaging* 1997;7:1084–93
47. Bruening R, Wu RH, Yousry TA, et al. **Regional relative blood volume MR maps of meningiomas before and after partial embolization.** *J Comput Assist Tomogr* 1998;22:104–10
48. Hakyemez B, Erdogan C, Ercan I, et al. **High-grade and low-grade gliomas: differentiation by using perfusion MR imaging.** *Clin Radiol* 2005;60:493–502
49. Eastwood JD, Provenzale JM. **Cerebral blood flow, blood volume, and vascular permeability of cerebral glioma assessed with dynamic CT perfusion imaging.** *Neuroradiology* 2003;45:373–76